ASME 2014 International Mechanical Engineering Congress & Exposition
IMECE 2014November 14-20, 2014, Montreal, Canada

IMECE2014-39991

COMBUSTION CHARACTERISTICS OF JOJOBA METHYL ESTER AS AN ALTERNATIVE FUEL FOR GAS TURBINE

Ali M.A. Attia
Mechanical Engineering Department, Benha
Faculty of Engineering, Benha University
13512 - Benha, Qalubia, Egypt
ali.attia@bhit.bu.edu.eg

Radwan M. El-Zoheiry
Mechanical Engineering Department, Benha
Faculty of Engineering, Benha University
13512 - Benha, Qalubia, Egypt
radwan85_bhit@yahoo.com

Hesham M. El-Batsh
Mechanical Engineering Department, Benha
Faculty of Engineering, Benha University
13512 - Benha, Qalubia, Egypt
helbatsh@bhit.bu.edu.eg

Mohamed S. Shehata
Mechanical Engineering Department, Benha
Faculty of Engineering, Benha University
13512 - Benha, Qalubia, Egypt
m3ohamed4@yahoo.com

ABSTRACT

The strengthened requirements of new emission norms and the limited fuel resources are the major challenges for researchers over the world. The use of biofuels produced from vegetable oil will be a promising solution. In this case, Jojoba oil comes from very surprising plant as its seed contains 40-60% of its weight as raw oil and grows in desert. The trans-esterification process is used to convert jojoba oil into a Jojoba Methyl Ester (JME). This study aims to characterize the flame of JME as an alternative fuel in the gas turbines. Using of the premixed flame resulted in higher combustion efficiency and low emissions. The premixed flames for liquid fuels can be realized via use of lean premixed pre-vaporized (LPP) combustion method. In this work the jet fuel and blends of jet-JME fuel (with JME volume faction of 10, and 20%) are burned with LPP technique keeping the same equivalence ratio as it is used for burning the base jet fuel to determine the possibility to use the fuel mixture without any modifications in a specific LPP combustor. The main results indicate that, as volume content of JME increase the NO_x emissions decrease to be lower than 10 ppm in case of B20. Moreover, the CO emission in case of B20 is higher than that of the jet fuel but at the end of the test section it does not exceed 0.15 %. In the same way, B20 produces higher UHC emissions than the jet fuel; however, at the end of the test section it does not exceed 80 ppm. So it can be concluded that blended Jojoba biodiesel can be used as an alternative fuel for jet fuel.

KEY WORD: Jojoba oil, trans-esterification, lean premixed pre-vaporized flames, temperature distribution, emissions.

1. INTRODUCTION

The necessity to protect human life throughout a continuously improving of the emission standards against the use of fossil fuels is faced with two major challenges for any nation; including the fast depletion of fossil fuel resources, and the accumulative environmental pollution [1]. At the same time, the gas turbine is widely used in different sectors including power generation, transportation and industrial applications where a large amount of fossil fuel is burned. These systems emit daily different toxic emissions as nitrogen oxides (NO_x), carbon monoxide (CO), unburned hydrocarbons (UHC) in addition to tons of carbon dioxides (CO_2); the major reason for greenhouse phenomenon. For reducing the level of toxic emissions, it is necessary to improve the fuel-air mixing as well as the combustion quality of the reactants. While to reduce the whole amount of CO_2 emissions it is necessary to replace the high carbon content fuels with those containing lower carbon contents. The first target can be realized by the use of low NO_x burners, and increasing the premixed part of the combustion process, while the second can be realized by use of those fuels based on renewable resources. In this case, the use of biofuel is a promising solution as an environmental friendly renewable substitute's fuel with a closed life cycle so that the cumulative CO_2 content will be null [2]. Different biodiesels have been recommended as gas turbine fuels [3, 4, and 5]. The liquid biofuels are commonly called biodiesel; as their physical properties approach those of petrol diesel. The biodiesel price depends mainly on the cost of the feedstock which represents more than 75% of the biodiesel total cost [2, 5, 7, and 8].

Therefore, the selection of the suitable feedstock for biodiesel production is a very important step to make biodiesel applicable in the commercial mode. In general, biodiesel feedstock can be divided into four main categories; including edible vegetable oils (such as canola, soybean, peanut, sunflower, palm and coconut oil), nonedible vegetable oils (such as Jojopa and Jatropha curcas), waste or recycled oils, and the animal fats ([6] and [8]). Traditionally, biodiesel has been produced from edible oils due to their low free fatty acids. However, the use of edible oils as feedstock for biodiesel production results in additional nutrition problems related to the food versus fuel issues leading to food crises. On the other hand, the use of non-edible oils may significantly reduce the cost of biodiesel production especially in poor countries which can barely afford the high cost of edible oils [5 and 7]. Moreover the oils from the non-edible resources are, as a rule, unsuitable for the human usage due to the presence of toxic compounds [5]. Thus, focus should be shifted towards the use of non-edible resources as biodiesel feedstocks. These oils are not only suitable for human nutrition but also can grow in the barren lands and/or need waste water [2, 5 and 7]. Jojoba oil appears to be one of these recommended vegetable oils for biodiesel production [9]. Jojoba plant is a shrub that grows very well in deserts and its cake is the solid part produced upon processing of the jojoba seeds for oil extraction [10]. Moreover, Jojoba plant lives for more than one hundred and fifty years and has unique properties as its seeds contain about 40 – 50 wt. % as raw oil–wax [10-12]. For these features of jojoba oil, it is expected to be an attractive feedstock for biodiesel production [12 and 17]. In this direction, the Egyptian jojoba oil (GREEN GOLD) seems to be a proper choice for biodiesel production due to its availability in Egypt, its low prices (0.8 €/kg), and its low chemical reactivity [14].

The modern gas turbines have two major challenges for development; including improving their thermal efficiency and reducing their emission level of CO and NO_x [3]. Thermal efficiency can be improved by considering the fuel combustion to reduce the energy loss due to incomplete mixing of fuel with air that usually burns in a diffusion mode. In this case, the use of premixed combustion will ensure the best economic use of the available fuel and so the maximum thermal efficiency. Regarding the reduction of emission level, different methods to prevent the formation of high temperature spots and to improve the fuel-air mixing have been recommended [3]. Among of these methods, the use of Lean Premixed Pre-vaporization (LPP) concept realizing at the same moment both the use of premixed flame as well as the use of lean mixture and so it represents the ultimate solution in this regard [3]. The LPP concept is based on operating the combustor at low equivalence ratio and supplying the combustor with a homogeneous combustible mixture. As a result of that, the combustion process proceeds at a uniformly low temperature, eliminates the droplet combustion and very little NO_x is formed [3]. For this reasons the LPP will be used in this research.

Generally, the behavior of the NO_x emission in the biodiesel combustion is not clear. There are many researches recorded a NO_x reduction with the use of biodiesel [5, 17, 18, and 19]. On the other hand, other researches cited that the NO_x emission increases with the use of biodiesel [4, 15, and 16]. Therefore, a study on the flame structure and the combustion characteristics of the biodiesel is necessary to get better understanding about this discrepancy. At the same time, the research regarding the combustion of the biodiesel in the LPP combustors has a shortage especially for biodiesel produced from jojoba oil. Therefore, this study is conducted in a LPP combustor.

This work is directed to study the effect of JME as a blend on the flame structure of jet fuel in a laboratory research lean premixed pre-vaporized combustor.

2. MATERIALS AND METHODS

The first step in this study is the preparation of the biodiesel from the raw jojoba oil. After that, JME is mixed with jet fuel and burned within a lean premixed pre-vaporized combustor with a swirl burner tip to study the combustion characteristics of the predefined fuel blend. The combustion characteristics have been determined as a function of temperature and emission distribution across the flame zone. The raw Jojoba oil is converted to Jojoba Methyl Ester (JME) via a trans-esterification process; a chemical reaction between methanol and raw Jojoba oil in the presence of catalyst of calcium hydroxide (KOH). The following section will explain the trans-esterification process of the JME.

2.1. Trans-esterification process

The raw Jojoba oil used in the present work is commercially produced by the Egyptian Natural Oil Company and supplied with technical specifications in comparison with the corresponding values reported in the literature as presented in Table 1 [31]. The methanol used in the preparation process of purity > 99.8% is supplied by Gomhoria Co and the catalyst used (KOH) has a purity > 85%.

The alcohol and catalyst concentrations and procedure used in the trans-esterification process are attained from the previous works to receive JME with minimum viscosity and acceptable yield [12-14]. In the present work, JME is received via trans-esterification following this procedure:

1- An l liter of raw jojoba oil is slowly heated within a water bath up to 60 °C while it is stirred mechanically with 600 rpm.
2- A 0.5 wt. % KOH from the raw oil is solved within 300 ml methanol forming methoxide. The amount of methanol used in this process will give the methanol to raw oil molar ratio of 6:1.
3- After that the prepared methoxide is added to the heated oil in two stages while stiring at a speed of 600 rpm. Firstly 75% of the solvent was added while the remaining amount is added after 10 minutes. During the reaction time, the mixture temperature is held constant at 60±1 °C.
4- After 2 hours from the starting of the reactants, the product is left in a separating funnel for 12 hours. During this period the product is separated in two layers; the upper layer

contains JME and the lower contains glyceride with remaining impurities of catalyst.

5- To accelerate the separation process, the product is washed with warm water from 4 to 5 times until a clean water is observed.
6- Finally the produced methyl ester was heated up to 100 ˚C in order to eliminate the remaining non-reacted methanol or washing water.

After that, the physical and chemical properties of the produced JME and the jet fuel that will be used in the present work have been determined as tabulated in Table 2.

Table 1 Technical specifications of the used jojoba oil compared with that used by Surname [8]

Characteristic	Current Jojoba oil	Oil used by [8]
Specific gravity at 25 º C	0.863	0.861
Flash point CS cc 9a-48, º C	295	275
Freezing point, º C	10.6 – 7.0	***
Melting points, º C	6.8 – 7.0	***
Boiling point at 1 am under N_2, º C	398	***
Kinematic viscosity at		
Cannon-Fenske, 25 º C, cSt.	50 cSt	***
Cannon-Fenske, 100 º C, cSt.	27 cSt	**
Viscosity index	232	****
Iodine value, g/100g	82	81
Average molecular weight, kg/K.mole	606	***
Heat of fusion by calorimatry, cal/g	21	***
Fire Point, ºC	338	322
Cetane number	53.5	***

Table 2 Properties of the JME and those of jet fuel

Property	Test method	JME	Jet
Specific gravity at 15°C	ASTM D-1298	0.8645	0.797
Viscosity at 40°C, cSt	ASTM D-445	11.72	1.08
Calorific value, MJ/kg	ASTM D-240	44.866	43.465
Molecular weight, kg/kmol	****	350.73	148.025
Elemental analysis, % by mass:			
Carbon content	PerkinElmer 2400 Series II CHNS/O Elemental Analyzer	76.01	86.51
Hydrogen content		10.05	13.48
Sulfur content		0.3	Nil
Oxygen content		13.64	Nil
Nitrogen content		Nil	Nil
Boiling point at 1 atm	ASTM D-86	350	163

2.2. Experimental apparatus

The experiments have been conducted in a lean premixed pre-vaporized (LPP) combustor (See Figures 1 – 3). In this experimental setup, cold air is supplied from a screw compressor through a pressure accumulator of 2 m^3 capacity. The compressor is allowed to switch on as the pressure fall between 8 and switch off when the pressure reaches 10 bar. Moreover, the air flow rate is adjusted by means of the gate valve while the upstream pressure is kept constant by means of the pressure regulator installed on the compressor oulet. This air is preheated using two Omega-AHPF inline air heaters. The supplied voltage to heaters is regulated by variable AC transformer (variac) to control the temperature of the pre-defined flow rate. The fuel is supplied from a pressurized fuel tank through a pressure atomizer nozzle (Delvan, 0.5 gph, 30°W). The fuel flow rate is regulated by controlling the tank pressure. In this way the fuel tank is pressurized by the compressed air and the pressure is controlled by the pressure regulator. The fuel nozzle is calibrated against the tank pressure to define the nozzle fuel flow rate for both base fuel and blended fuels. Furthermore the fuel flow rate is measured by a calibrated Dwyer-DR (model DR224632) rotameter in addition to the previous calibration of the fuel nozzle at the specific operating pressure. The fuel is injected into the stream of preheated air throughout a steel mixing pipe. Then a free length of 1 m of this pipe before burner is used to achieve good mixing between air and injected fuel and to ensure fuel fully vaporization before their combustion. To stabilize the developed flame, the burner is integrated with axial swirler. The swirler is consisted of 8 axial vanes mounted at the siwrler hub at angle (θ) of 45°. The swirl number in this case is 0.78 which is selected to match the cited values in the literature for low swirl burner [20-24]. For an annular swirler with constant vane angle θ, the swirl number is given as in equation 1. so, the swirl number is calculated by equation 1 [3] (see Figure 1 for swirler details):

$$S_N = \frac{2}{3}\left(\frac{1-\left(D_{hub}/D_{SW}\right)^3}{1-\left(D_{hub}/D_{SW}\right)^2}\right)\tan\theta \qquad \text{Equation 1}$$

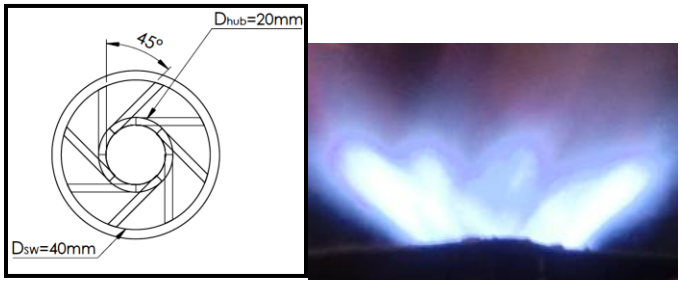

Figure 1 Swirler dimensions and a photo for jet fuel flame with Φ =0.87

The tip of the swirler is aligned with the dump plan of the combustion chamber as shown in Figure 2 and Figure 3. The dimensions of the combustion chamber has been selected to match the dimensions of similar combustors used for flame study in the literature [25-28]. It can be concluded from these materials that, the combustion chamber diameter is four times that of the burner ($D_{C.C.}$ = 4 D_B) and the length of the combustion chamber is greater than ten times the burner diameter ($L_{C.C.}$ > 10 D_B). Therefore, the steel combustion chamber of diameter 150 mm and length of 500 mm based on burner diameter of 38 mm has been used. Full details of the confined tube and mixing section are available in Figure 3. In this work, the flame is ignited by means of two steel electrodes and high voltage transformer as that used in commercial boilers.

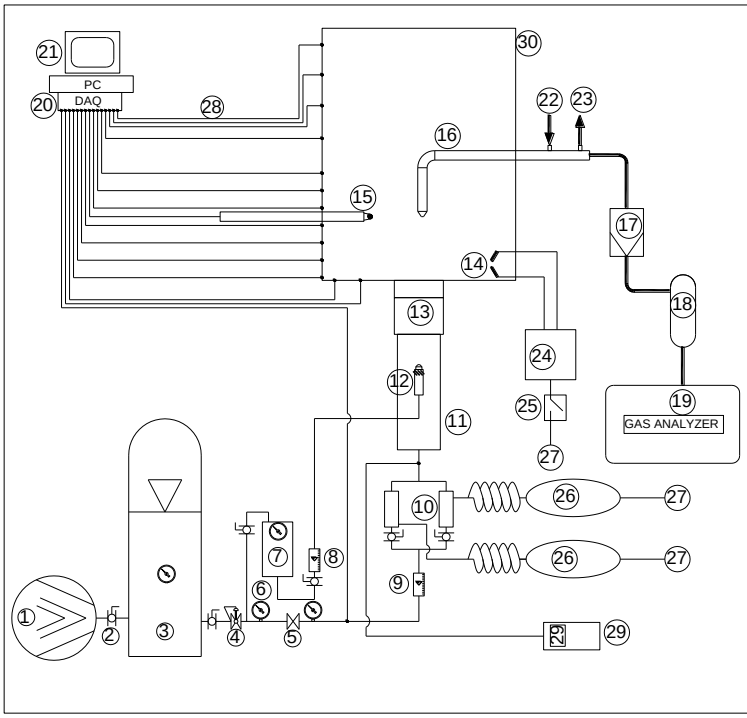

Symbol / Abbreviation	Description
①	Screw compressor
②	Ball valve
③	Pressure Accumulator
④	Pressure Regulator
⑤	Gate Valve
⑥	Pressure Gauge
⑦	Fuel Tank
⑧	Fuel Rtoameter
⑨	Air Rotameter
⑩	Inline Air Heater
⑪	Mixing Steel Pipe
⑫	Pressure Atomizer
⑬	Burnner
⑭	Spark Electrodes
⑮	Type R Thermocouple
⑯	Sampling Probe
⑰	Filter
⑱	Condensate Water filter
⑲	Gas Analyzer
⑳	Data Acquisition
㉑	Personal Computer
㉒	Cooling Water In
㉓	Cooling Water Out
㉔	Transformer
㉕	Switch
㉖	Voltage Variac
㉗	Electrical Source
㉘	Type K Thermocouple
㉙	Digital Thermometer
㉚	Combustion Chamber

Figure 2 Schematic drawing for the experimental test rig

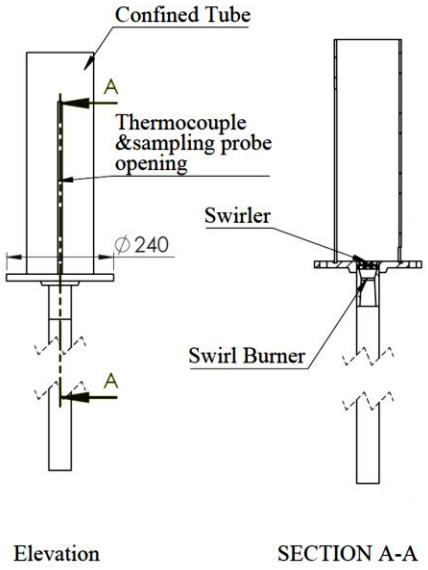

Figure 3 Confined tube detailed dimensions

During all experiments the equivalence ratio is kept constant by adjusting the fuel and air flow rate as requested according to the fuel blend. It is necessary to inject the fuel blends at higher pressure to withstand the pressure loss attained from the viscosity increase of these blends compared with the viscosity of jet fuel. Furthermore, in order to check the availability of substitute jet fuel with JME blended fuel in the same combustor without modifications, the inlet air temperature is kept constant for all experiments. The temperature is monitored by thermocouple type K in conjunction with digital thermometer (AZ-8852 with resolution of 1 °C) digital thermometer downstream of the electrical heaters. The overall experimental program is summarized in Table 3.

Table 3 Test condition in the experiments

Test condition	B0	B10	B20
Fuel injection pressure, bar	7	9	9
Fuel flow rate, kg/hr.	1.28	1.41	1.56
Air flow rate, kg/hr.	21.08	22.96	24.75
Equivalence ratio	0.87	0.87	0.87
Air inlet temperature, °C	160	160	160

In order to achieve the goals of the present work, the axial and radial distribution of the flame temperature and species concentrations are measured. Measurements are conducted at eleven vertical planes with five radial locations in each plane. These planes are at vertical distances from the burner tip equal to 0, 10, 20, 30, 40, 50, 60, 80, 100, 120, and 140 mm, while the radial locations of the measurements are located at 0, 5, 10, 15, and 20 mm from the burner centerline.

The flame temperature was measured using thermocouple type R (Pt/Pt-13%Rh). At the same time, thirteen type K thermocouples are mounted at different locations along the combustor wall in order to measure the wall temperatures. These wall temperatures are used to correct the flame temperature thermocouple reading against heat transfer losses by radiation from its bead to the combustor wall, according to the procedure recommended by Dent [32]. The different thermocouple readings are acquired automatically using Data Acquisition Card (Model NI USB-9213) and LabView signal express software installed on a PC.

To measure the local concentration of different species (CO, CO_2, O_2, UHC and NO_x) water cooled isokinetic sampling probe in conjunction with AVL Dicom 4000NO_x gas analyzer are used. The CO, CO_2, and UHC concentrations are measured using infrared detectors (NDIR) based on the attenuation of the infrared wavelength beam specific to each species [29]. While NO_x and O_2 concentrations are measured using electrochemical detectors. Furthermore an inline filter and water condenser are used before passing the flue gases through the gas analyzer in order to eliminate the contents of particles and moisture. In order to move the type R thermocouple and the sampling probe on the discrete points, a two dimensional traverse mechanism is used.

2.3. Data analysis

After measuring the flame temperature and species concentrations, the obtained data were analyzed as following:

1. The NO_x concentrations are corrected to 15% O_2 in order to eliminate the effect of dilution air on the emission comparison
2. The output of the UHC channel in the gas analyzer always related to the hexane, therefore the UHC readings are corrected to the used fuel as in equation 2 [29].

$$\boldsymbol{UHC_{fuel} = UHC_{measured} \times \frac{Mw_{hexane}}{Mw_{fuel}}} \qquad \text{Equation 2}$$

3. The flame temperature is measured by recording 3000 samples for each point with a rate of 100 samples per second. After that the average value of these samples is calculated.
4. The value of the temperature is corrected for radiation error.
5. All this data is plotted using Sigma plot and table curve programs.

3. RESULTS AND DISCUSSION

The experiments related to the jet fuel combustion are performed initially, and then different blended fuels of JME and jet fuel are used according to the experimental program summarized in Table 3.

Figure 4 shows the temperature distribution due the combustion of different fuels. The jet fuel combustion is discussed initially as it is the base fuel. As the burner contains a central solid bluff-body (20 mm diameter) in conjunction with the swirled flow, there will be a recirculation zone at the burner center where the flame is stabilized. In this recirculation zone adjacent the bluff-body a portion of the hot combustion products is entrained and recirculated to mix with the incoming air-fuel premixed mixture. This is accomplished by a higher temperature zone near the edge of the bluff-body where the hot recirculated products exist. Away from the bluff-body edge to the center, the recirculated hot products keep high temperature. On the other side from the bluff-body edge towards the combustor wall, the temperature fall down gradually as shown on Figure 4 and in particular at the lower vertical plans. Furthermore as the vertical distance is increased while the intensity of the central recirculation zone is decayed and the flow becomes more homogeneous, the temperature variation with the radial distance is decreased, this attained after 80 mm from the burner tip. Thus at vertical distance around 30 mm, the maximum axial temperature due to jet fuel burning is obtained while beyond 80 mm the temperature is stabilized.

The biodiesel blend ratio affect the radial position at which the maximum temperature is obtained as well as the vertical distances where both maximum temperature and the stabilized temperatures are achieved, as shown in Figure 4. It can be noted that, at blend ratio of 20% (B20) a similar temperature distribution to that of jet fuel is observed. The resultant parameters from the mixing of biodiesel with jet fuel that influence the temperature distribution include heating value, oxygen content, mixture homogeneity, as well as the completeness of phase change of biodiesel before entering the flame zone. The heating values are similar for both base fuels, while the oxygen contents into JME will improve the reaction mechanisms within the flame zone. The last two parameters are attained as the biodiesel exhibits a completely different viscosity and volatility compared with the corresponding properties for jet fuel; viscosity is greater than ten times while the boiling point is more than twice times (See Table 2). As the blend ratio is increased, there will be a great chance to have aerosols of biodiesel in phase change not due to boiling but due to surface evaporation as the preheat temperature still beyond its boiling point. Accordingly, the incoming mixture into the flame zone may have spots containing very rich mixture (nonhomogeneous mixture) or even very fine aerosols of biodiesel (forming heterogeneous zones), and these spots and aerosols should be significant as the blend ratio is increased. These zones should give higher temperature near the burner tip.

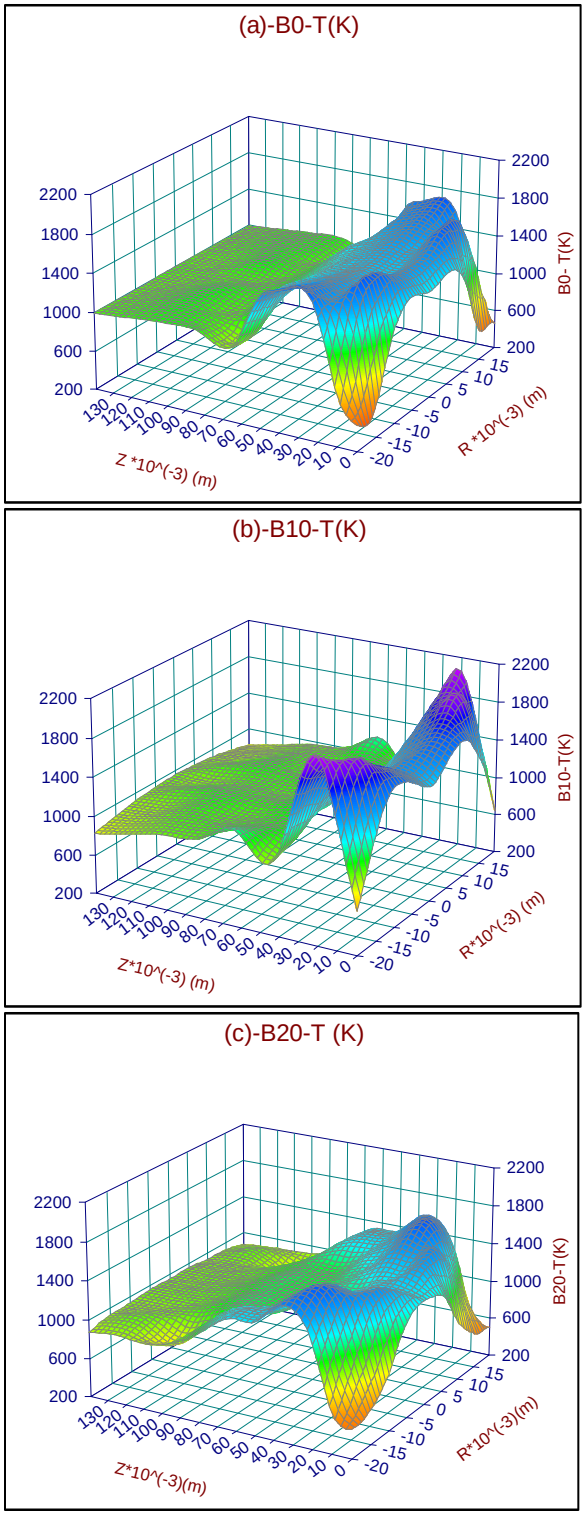

Figure 4 B0, B10 and B20 in flame temperature distribution

At 10% blend ratio (B10), the fuel aerosols may be not exist, but the spots of rich mixture may exist, this is why the flame temperature in case of B10 is higher than that of jet fuel (B0) especially near to the burner tip. However, at the end of axial distance a closure temperature distribution is observed (see Figure 4). Additional reason for this difference in temperature distribution especially near burner tip can be owing to fuel chemical structure. As the double bond in the biodiesel and the improved chemical reaction rates due to oxygen contents will increase the flame temperature that may be partially compensated by the lower carbon contents which should reduce the flame temperature. Beyond the burner tip, after 40 mm, the spots of nonhomogeneous and/or heterogeneous mixture are disappeared and so after this level the combustion becomes more homogeneous and the flame temperature becomes closer to that of the jet fuel no matter the blending ratio. The slight decrease in the combustion products at the end of axial locations can be owing to the use of lower energy contents to maintain the mixture equivalence ratio while biodiesel already containing oxygen. This is why for B20 the flame temperature is observed to be lower than that of B10. However, for B20 the degree of non-homogeneity and heterogeneity are dominant, the location of maximum temperature is attained at further vertical distance than that for B10 to allow more time for complete evaporation, so the flame temperature of B20 reaches the steady state at a plan higher than that of B10 and B0.

The similar flame temperature distribution between B0 and B20 implies that, the mixture containing JME up to 20% can be used as fuel substitute the jet fuel without any change in the combustor design as the combustor pattern factor does not changed. This in turn means the preservation of huge investments done in the development of the existing combustors.

The formed emissions in the premixed combustion are mainly function of the local equivalence ratio, temperature and turbulence intensity. Figure 5 shows the CO concentrations throughout the studied flames including Jet fuel, B10, and B20. Burning of the JME-jet fuel blends in the LPP combustor with the same inlet temperature produces a comparable CO concentrations with that of the jet fuel. From Figure 5 it is noted that, the CO concentration produced from the jet fuel combustion is almost constant along the combustor axis and decreased as the radial distance from the burner centerline is increased until reaches the minimum value at the farthest point from the burner centerline. This phenomena is due to the burner structure which has a solid region at the center and the recirculation zone is formed at the center of the burner. Additional reason is conducted with temperature distribution, at high local temperature the dissociation reactions of CO_2 to form CO are significant rather than at lower temperature at end of the flame. Furthermore, as the percentage of the JME is increased in the jet-JME blends, the CO is increased which can be owing to the formation of rich spots as well as the possibility to have heterogeneous mixture due to poor vaporization of the lower volatile fuel. Thus the injection of the fuel blends in air at fixed temperature as that used when jet fuel is used leads to less pre-vaporizing of the fuel and so more CO emission is formed rather than the CO emission due to homogenous combustion as in the case of pure jet fuel. But as the vertical distance is increased, the mixture homogeneity is improved and the local

temperature is reduced and so CO emissions are decreased approaching the concentrations obtained from jet fuel combustion. This CO can be reduced by simply increase the inlet temperature to be closer to the boiling point of the JME.

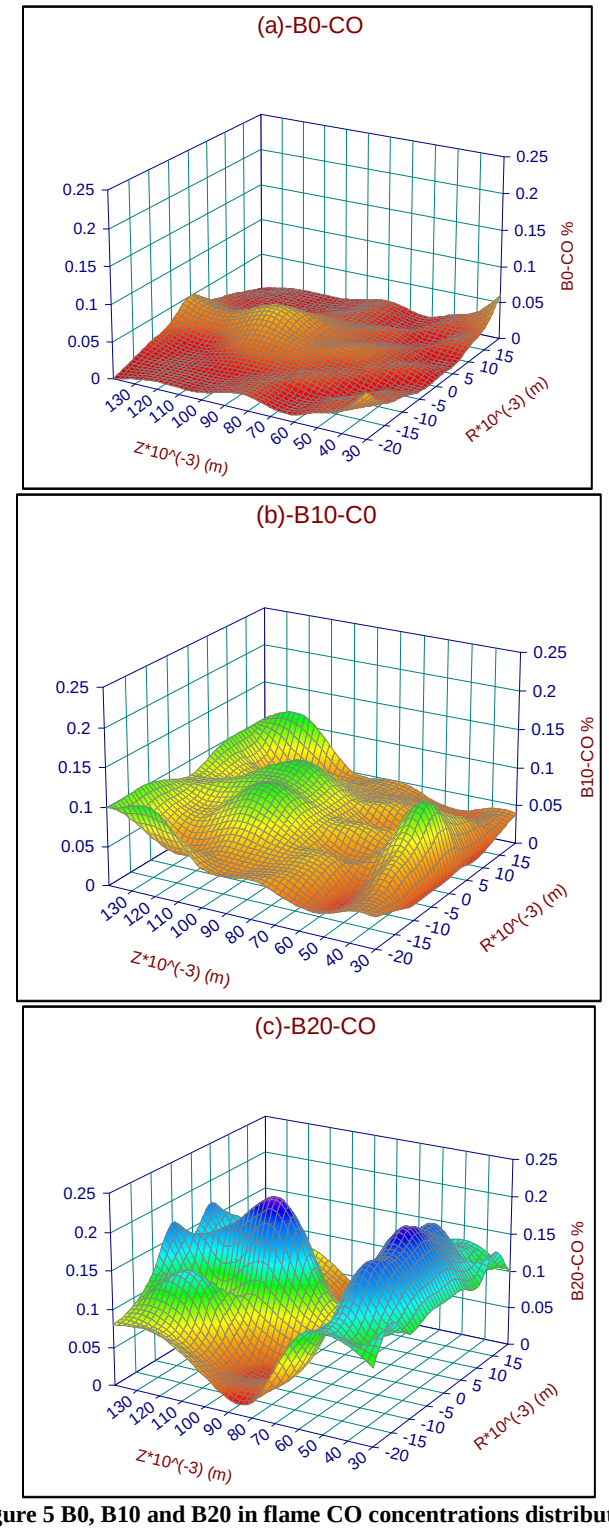

Figure 5 B0, B10 and B20 in flame CO concentrations distribution

The UHC concentration throughout the flame is controlled by good mixing of reactants (gas mixture homogeneity), the fuel degradation mechanism as well as the mixture strength. Its level will be high for nonhomogeneous, rich mixture combustion of heavy fuels. As the UHC are usually formed during fuel cracking, the high temperature will play a great influence on their oxidation to form non-pollutant emissions. Figure 6 shows the UHC emissions distribution for the jet fuel and blends. This figure reveals that the UHC emission from the jet fuel combustion is increased with the vertical distance above the burner tip due to the effect of temperature. On the other hand, in case of B10, the UHC emissions are increased with vertical distance till reaches the maximum value in most radial locations after 110 mm from the burner tip due to the non-homogeneity and the possibility to have a heterogeneous mixture. After that, the UHC takes to decrease with the vertical distance to reach the minimum value at the end of the test section.

In case of B20 and in the flame core, the UHC behaves as in case of B10 as shown in Figure 6. Far away from the flame core, the UHC in case of B20 almost constant along the test section length at each radial location. Furthermore, Figure 6 revealed that, the UHC produced from B10 combustion is lower than that in case of B0 and B20. This decrease of the UHC in case of B10 can be owing to the positive effect of the oxygen content that competes the negative effect of mixture non-quality. The oxygen contents generally improve the reaction kinetics and so improving the combustion process leading to a remarkable reduction of the UHC formation. While in case of B20 the negative effects are higher leading to increase the UHC formation than that of B10. These effects include the poor mixing of reactants as well as the increase of carbon double bonds in case of B20 compared with the case of B10 and B0. From another point of view, at the end of the test section and in the worst case, the UHC produced from B20 was higher than that of B0 by not more than 15 ppm which is not a big difference. Furthermore as the UHC in case B0 increases with the vertical distance and in case of B20 remains constant or falls down, it is observed that at higher levels the UHC from B20 is lower than that of B0.

The results presented in Figure 7 revealed that, the CO_2 emissions from the blends and that from the jet fuel have the same behavior. Furthermore it is noted that, at the farthest point from the burner the percentage of CO_2 produced from the blends are very close to that from the jet fuel combustion. But in contrast to the fossil fuels such as the jet fuel, the use of biodiesel does not add any CO_2 to the atmosphere, it just recycles what was already there. So the use of biodiesel as a blend with the fossil fuel actually reduce the net value of the CO_2 added to the atmosphere and so reduces the greenhouse effect.

Figure 8 represents the NO_x distributions in case of jet fuel and JME-jet fuel blends. In this figure, the NO_x is referenced to 15% oxygen on a dry basis in order to remove ambiguity during the comparison of the different sets of experimental data. The results presented in this figure reveals that, in most locations

within the combustor the NO_x emissions produced by the blends are lower than that those produced by the jet fuel. Furthermore, from this figure, a reduction in the NO_x emission with the increase of the JME content in the blends can be noted in some locations. In addition to that, the NO_x emissions from the jet fuels at the end of the test section are less than 15 ppm. While in case of B20 for all radial locations the NO_x emission is below 10 ppm, this challenge in the new gas turbine combustion technologies to achieve 10 ppm NO_x is realized by means of LPP using blends fuels containing biodiesel fraction. In most combustion applications where fuel has low nitrogen contents, the thermal NO_x is the major NO_x formation mechanism for temperature above 1850 K [3]. Therefore as the flame temperature in most locations is lower than this limit (1850 K), tendency of thermal NO_x formation is reduced and the overall NO_x emission is reduced drastically. Furthermore, supplying the combustor with homogeneous mixture eliminates the droplet combustion which in turn avoiding the local high temperature thus the NO_x emissions are reduced.

4. CONCLUSION

In this study, a biodiesel produced from jojoba raw oil by the trans-esterification process has been added to jet fuel forming blended fuel in purpose of introducing an alternative fuel for the jet fossil fuel. An experimental setup to realize the Lean Premixed Pre-vaporized (LPP) concept has been constructed with selected dimensions to match the similar setups used for flame studies, here the flame is stabilized by the use of swirl burner. This work is aimed to study the effect of mixing JME with jet fuel on the flame structure compared with that due to conventional jet fuel combustion without changing in the existing combustor at the same equivalence ratio. The testes are performed by burning the jet fuel, B10, and B20 biodiesel-jet blends in a LPP combustor, and the following conclusions have been raised:

1- The flame temperature distributions for different tested fuels are similar especially in case of B0 and B20.
2- The combustion of the blends especially B20 relative to jet fuel produce higher CO, slightly higher UHC, and comparable values of CO_2 emissions.
3- The use of biodiesel blended fuels in conjunction with the LPP combustion technology remarkably reduces the NO_x emission lower than 10 ppm.
4- Thus, the replacement of the jet fuel with blended biodiesel-jet fuel up to 20% by volume biodiesel does not need any changes in the combustor design as there is no significant change in the temperature distribution with acceptable emission level.

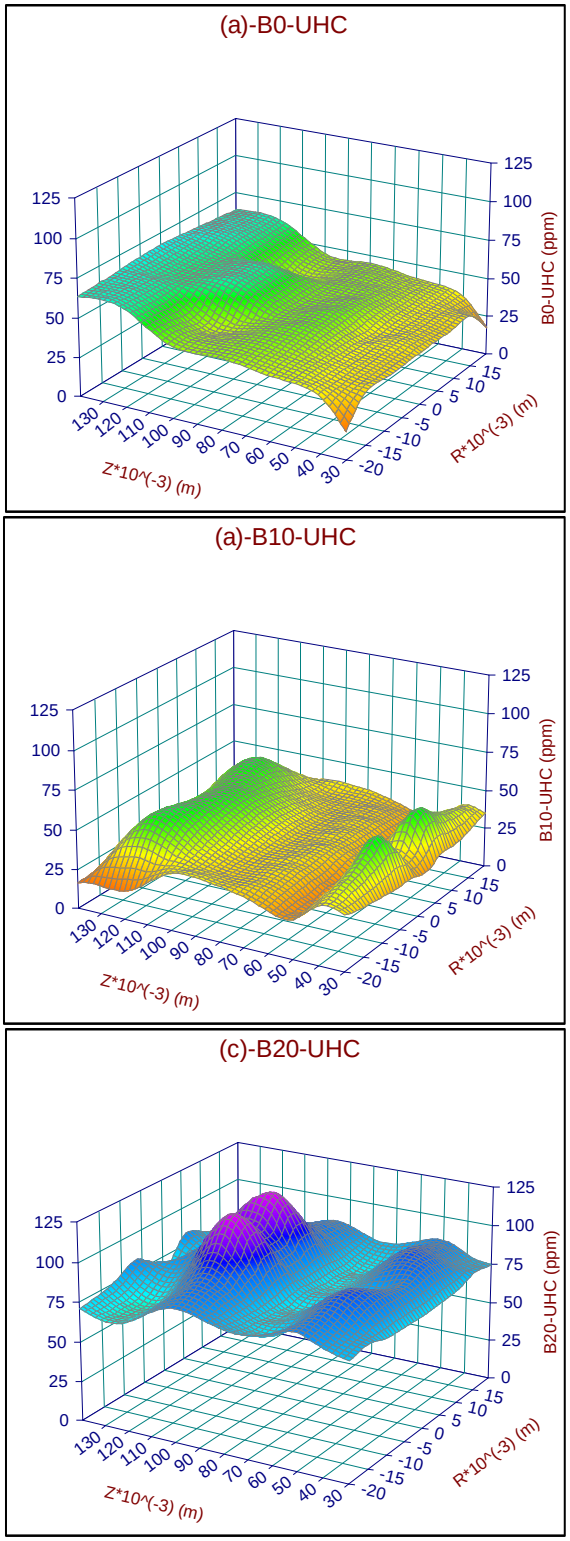

Figure 6 B0, B10 and B20 in flame UHC concentrations distribution.

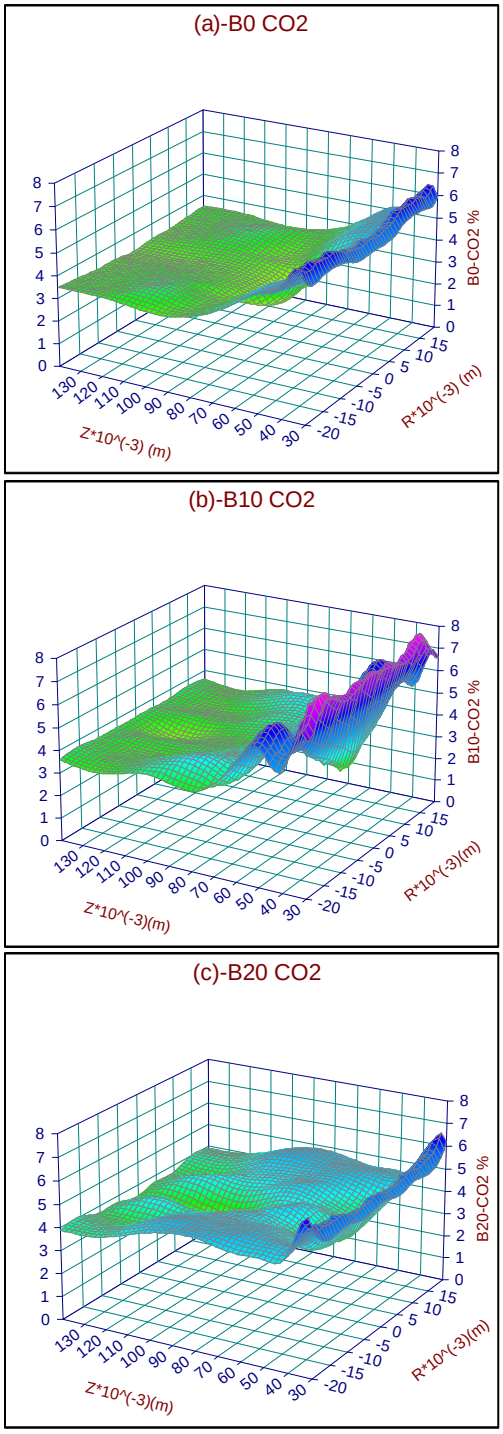

Figure 7 B0, B10 and B20 in flame CO_2 concentrations distribution.

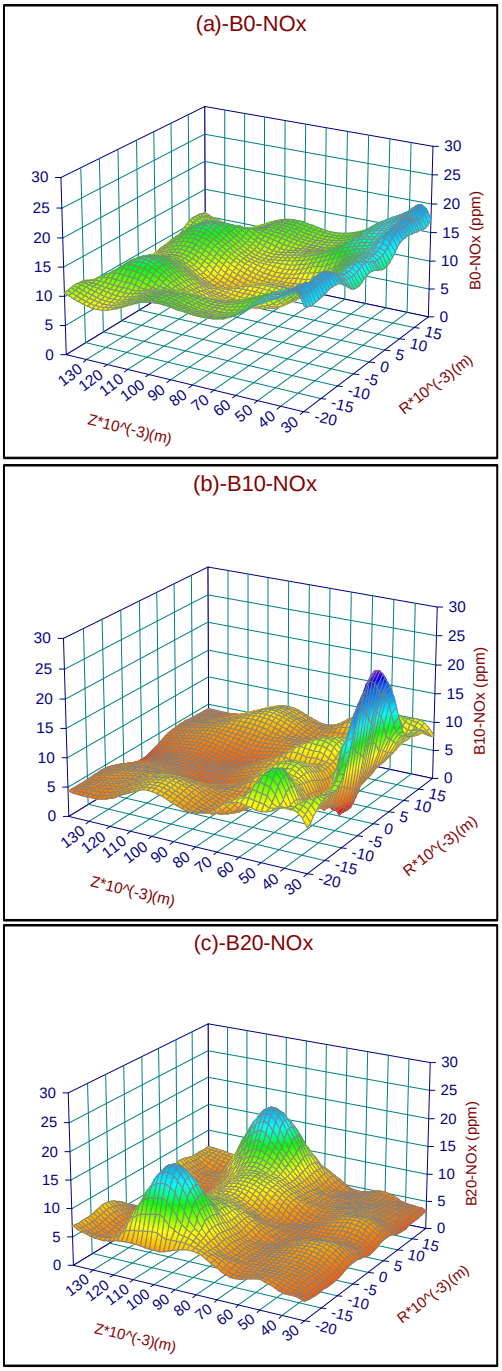

Figure 8 B0, B10 and B20 in flame NO_x concentrations distribution.

REFERENCES

[1] Mujeebu M. A., Abdullah M.Z., Abu Bakar M.Z., Mohamad A.A., Muhad R.M.N., Abdullah M.K. Combustion in porous media and its applications – A comprehensive survey. Journal of Environmental Management 2009; 90: 2287–2312.

[2] Demirbas A. Political, economic and environmental impacts of biofuels: A review. Applied Energy 2009; 86: S108-S117.
[3] Lefebvre A.H., Ballal D.R. Gas turbine combustion. Third edition.
[4] Bolszo C.D., McDonell V.G. Emissions optimization of a biodiesel fired gas turbine. Proceedings of the Combustion Institute 2009; 32: 2949-2956.
[5] Habib Z., Parthasarathy R., Gollahalli S. Performance and emission characteristics of biofuel in a small-scale gas turbine engine. Applied Energy 2010; 87: 1701-1709.
[6] Rutz D., Janssen R. Biofuel technology handbook. 2007
[7] Atabani A.E., Mahlia T.M.I., Masjuki H.H., Badruddin I. A. A comparative evaluation of physical and chemical properties of biodiesel synthesized from edible and non-edible oils and study on the effect of biodiesel blending. Energy 2013; 58: 296-304.
[8] Mofijur M., Atabani A.E., Masjuki H.H., Kalam M.A., Masum B.M. A study on the effects of promising edible and non-edible biodiesel feedstocks on engine performance and emissions production: A comparative evaluation. Renewable and Sustainable Energy Reviews 2013; 23: 391-404.
[9] Selim M.Y.E., Radwan M.S., Elfeky S.M.S. Combustion of jojoba methyl ester in an indirect injection diesel engine. Renewable Energy 2003; 28:1401-1420.
[10]Al-Widyan M.I., Al-Muhtaseb M.A. Experimental investigation of jojoba as a renewable energy source. Energy Conversion and Management 2010; 51:1702-1707.
[11] Selim M.Y.E. Reducing the viscosity of Jojoba Methyl Ester diesel fuel and effects on diesel engine performance and roughness. Energy Conversion and Management 2009; 50: 1781-1788.
[12] Radwan M.S., Ismail M.A., Elfeky S.M.S., Abu-Elyazeed O.S.M. Jojoba methyl ester as a diesel fuel substitute: Preparation and characterization. Applied Thermal Engineering 2007; 27: 314-322.
[13] Shah S.N., Sharma B.K., Moser B.R., Erhan S.Z. Preparation and evaluation of jojoba oil methyl esters as biodiesel and as a blend component in ultra-low sulfur diesel fuel. Bioenerg. Res. 2010; 3: 214-223.
[14] Abdel Fatah M., Farag H.A., Ossman M.E. Production of biodiesel from non-edible oil and effect of blending with diesel on fuel properties. IRACST – Engineering Science and Technology: An International Journal (ESTIJ), ISSN 2012; 2: 2250-3498.
[15] Ng H.K., Gan S. Combustion performance and exhaust emissions from the non-pressurised combustion of palm oil biodiesel blends. Applied Thermal Engineering 2010; 30: 2476-2484.
[16] Lin Y., Wu Y.G., Chang C.T. Combustion characteristics of waste-oil produced biodiesel/diesel fuel blends. Fuel 2007; 86: 1772-1780.
[17] Jaime A.E.Jr., Parthasarathy R., Gollahalli S. Atomization and combustion of canola methyl ester biofuel spray. Fuel 2010; 89: 3735-3741.
[18] Ghorbani A., Bazooyar B., Shariati A., Jokar S.M., Ajami H., Naderi A. A comparative study of combustion performance and emission of biodiesel blends and diesel in an experimental boiler. Applied Energy 2011; 88: 4725-4732.
[19] Hashimoto N., Ozawa Y., Mori N., Yuri I., Hisamatsu T. Fundamental combustion characteristics of palm methyl ester (PME) as alternative fuel for gas turbines. Fuel 2008; 87: 3373-3378.
[20] Gupta A. K., Lewis M. J., Daurer M. Swirl Effects on Combustion Characteristics of Premixed Flames. Journal of Engineering for Gas Turbines and Power 2001; vol. 123/621.
[21] Kim K.T., Santavicca D.A. Interference mechanisms of acoustic/convective disturbances in a swirl-stabilized lean-premixed combustor. Combustion and Flame 2013; 160: 1441-1457.
[22] De A., Acharya S. Parametric study of upstream flame propagation in hydrogen-enriched premixed combustion: Effects of swirl, geometry and premixedness. International journal of hydrogen energy 2012; 37: 14649-14668.
[23] Tunçer O., Kaynaroğlu B., Karakaya M.C., Kahraman S., Yıldırım O.Ç., Baytas C. Preliminary investigation of a swirl stabilized premixed combustor. Fuel 2014; 115: 870-874.
[24] Owaki T., Umemura A. Premixed swirl combustion modes emerging for a burner tube with converging entrance. Proceedings of the Combustion Institute 2007; 31: 1067-1074.
[25] Sinha A., Ganguly R., Puri I.K. Control of confined nonpremixed flames using a microjet. International Journal of Heat and Fluid Flow 2005; 26: 431-439.
[26] Birbaud A.L., Durox D., Ducruix S., Candel S. Dynamics of confined premixed flames submitted to upstream acoustic modulations. Proceedings of the Combustion Institute 2007; 31: 1257-1265.
[27] Palies P., Duroxa D., Schuller T., Morentonb P., Candel S. Dynamics of premixed confined swirling flames. C. R. Mecanique 2009; 337: 395-405.
[28] Cuquel A., Durox D., Schuller T. Scaling the flame transfer function of confined premixed conical flames. Proceedings of the Combustion Institute 2013; 34: 1007-1014.
[29] AVL DiCom 4000. Operating Manual. Edition 03/2001.
[30] Turns S.R. An introduction to combustion concepts and applications, 2nd Ed., McGraw-Hill Book Co., 2000.
[31] N. El Moguy, Jojoba: The Green Gold Hope for the Egyptian Desert Development United Nations: Economic and Social Commission for Western Asia, Report of the Experts Group Meeting Manama (Bahrain), June2002.
[32] Dent T.J., Mesoscale power generation incorporating heat-recirculation, porous inert media, and thermoelectric modules. PhD thesis. The University of Alabama, Department of Mechanical Engineering. 2012

